Rethinking Rotated Object Detection with Gaussian Wasserstein Distance Loss

Xue Yang[1,2,4], Junchi Yan[1,2], Qi Ming[3], Wentao Wang[1], Xiaopeng Zhang[4], Qi Tian[4]

[1]Department of CSE, SJTU [2]MoE Key Lab of Artificial Intelligence, AI Institute, SJTU

[3]School of Automation, Beijing Institute of Technology [4]Huawei Inc.

SHANGHAI JIAO TONG UNIVERSITY

HUAWEI

ICML International Conference On Machine Learning

Introduction:

- Task: Design a novel multi-category rotation detector for small, cluttered and rotated objects.
- Challenges:
  - The inconsistency between metric and loss
  - Boundary discontinuity
  - Square-like problem
- Our main contributions：
  - We summarize three flaws in state-of-the-art rotation detectors, i.e. inconsistency between metric and loss, boundary discontinuity, and square-like problem, due to their regression based angle prediction nature.
  - We propose to model the rotating bounding box distance by Gaussian Wasserstein Distance (GWD) which leads to an approximate and differentiable IoU induced loss. It resolves the loss inconsistency by aligning model learning with accuracy metric and thus naturally improves the model.
  - Our GWD-based loss can elegantly resolve boundary discontinuity and square-like problem, regardless how the rotating bounding box is defined. In contrast, the design of most peer works are coupled with the parameterization of box.
- Codes:https://github.com/yangxue0827/RotationDetection

Proposed Approach

- Most of the IoU-based loss can be considered as a distance function. Inspired by this, we propose a new regression loss based on Wasserstein distance. First, we convert a rotating bounding box B(x,y,h,w,θ) into a 2-D Gaussian distribution N(m,∑).

$$
\begin{aligned}
\Sigma^{1/2} &= \mathbf{R}\mathbf{S}\mathbf{R}^{\top} \\
&= \begin{pmatrix} \cos\theta & -\sin\theta \\ \sin\theta & \cos\theta \end{pmatrix} \begin{pmatrix} \frac{w}{2} & 0 \\ 0 & \frac{h}{2} \end{pmatrix} \begin{pmatrix} \cos\theta & \sin\theta \\ -\sin\theta & \cos\theta \end{pmatrix} \\
&= \begin{pmatrix} \frac{w}{2}\cos^2\theta + \frac{h}{2}\sin^2\theta & \frac{w-h}{2}\cos\theta\sin\theta \\ \frac{w-h}{2}\cos\theta\sin\theta & \frac{w}{2}\sin^2\theta + \frac{h}{2}\cos^2\theta \end{pmatrix} \\
\mathbf{m} &= (x, y)^{\top}
\end{aligned}
$$

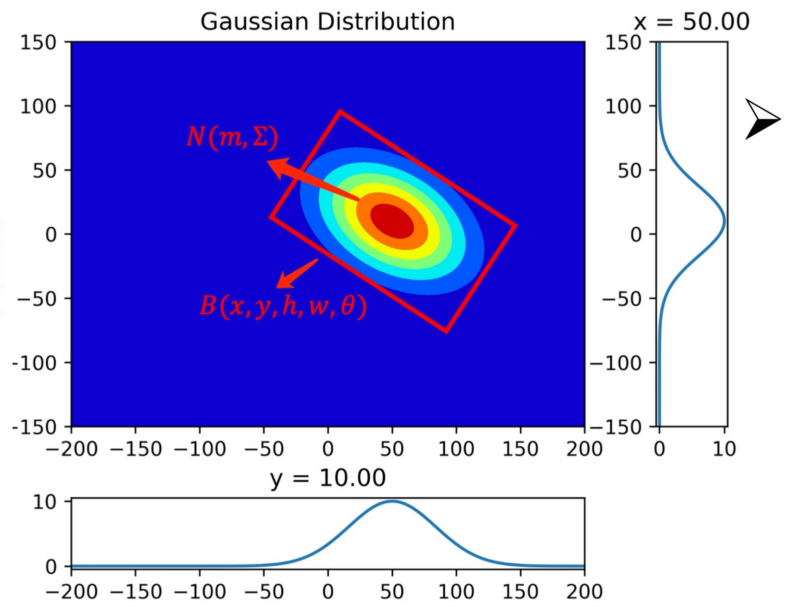

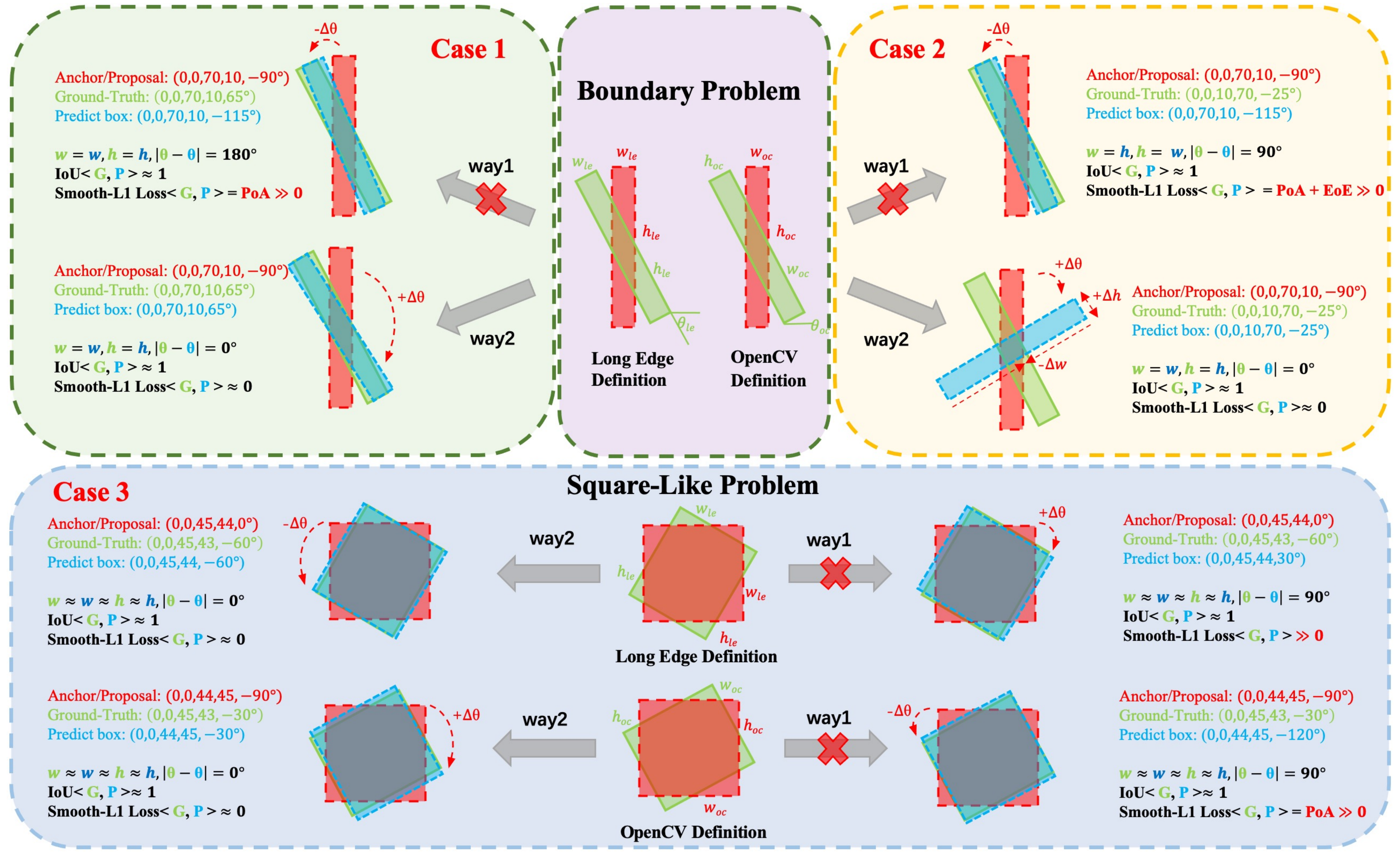

Figure 1. Boundary discontinuity under two bounding box definitions (top), and illustration of the square-like problem (bottom).

- GWD has the following properties to solve all the problems in Figure 1:

$$\textbf{Property 1: } \Sigma^{1/2}(w,h,\theta) = \Sigma^{1/2}(h,w,\theta-\tfrac{\pi}{2});$$

$$\textbf{Property 2: } \Sigma^{1/2}(w,h,\theta) = \Sigma^{1/2}(w,h,\theta-\pi);$$

$$\textbf{Property 3: } \Sigma^{1/2}(w,h,\theta) \approx \Sigma^{1/2}(w,h,\theta-\tfrac{\pi}{2}), \text{ if } w \approx h.$$

- The Wasserstein distance between two probability measures can be expressed as fellow:

$$d^2 = \|\mathbf{m}_1 - \mathbf{m}_2\|_2^2 + \mathbf{Tr}\left(\boldsymbol{\Sigma}_1 + \boldsymbol{\Sigma}_2 - 2(\boldsymbol{\Sigma}_1^{1/2}\boldsymbol{\Sigma}_2\boldsymbol{\Sigma}_1^{1/2})^{1/2}\right)$$

- Gaussian Wasserstein Distance Regression Loss：

$$L = \frac{\lambda_1}{N}\sum_{n=1}^{N} obj_n \cdot L_{gwd}(b_n, gt_n) + \frac{\lambda_2}{N}\sum_{n=1}^{N} L_{cls}(p_n, t_n)$$

$$L_{gwd} = 1 - \frac{1}{\tau + f(d^2)}, \quad \tau \geq 1$$

Experiments:

- Ablation study for GWD on three dataset.

Method	Box Def.	Reg. Loss	Dataset	Data Aug.	mAP$_{50}$
RetinaNet	D_{oc}	Smooth L1	HRSC2016	R+F+G	84.28
	D_{oc}	GWD			**85.56 (+1.28)**
	D_{oc}	Smooth L1	UCAS-AOD		94.56
	D_{oc}	GWD			**95.44 (+0.88)**
	D_{oc}	Smooth L1	DOTA	F	65.73
	D_{oc}	GWD			**68.93 (+3.20)**
	D_{le}	Smooth L1			64.17
	D_{le}	GWD			**66.31 (+2.14)**
R^{3}Det	D_{oc}	Smooth L1			70.66
	D_{oc}	GWD			**71.56 (+0.90)**

- Ablation study for GWD on two scene text datasets.

Method	Reg. Loss	Dataset	Data Aug.	Recall	Precision	Hmean
RetinaNet	Smooth L1	MLT	F	37.88	67.07	48.42
	GWD			44.01	71.83	**54.58 (+6.16)**
	Smooth L1	ICDAR2015		71.55	68.10	69.78
	GWD			73.95	74.64	**74.29 (+4.51)**
	Smooth L1		R+F	69.43	81.15	74.83
	GWD			72.17	80.59	**76.15 (+1.32)**
R^{3}Det	Smooth L1		F	69.09	80.30	74.28
	GWD			70.00	82.15	**75.59 (+1.31)**
	Smooth L1		R+F	71.69	79.80	75.53
	GWD			73.95	80.50	**77.09 (+1.56)**

- Peer method comparison.

Base Detector	Method	Box Def.	IML	BD		SLP	Tranval/Test									Train/Val		
				EoE	PoA		BR†	SV†	LV†	SH†	HA†	ST‡	RA‡	7-mAP$_{50}$	mAP$_{50}$	mAP$_{50}$	mAP$_{75}$	mAP$_{50:95}$
RetinaNet	-	D_{oc}	✓	✓	✓	×	42.17	65.93	51.11	72.61	53.24	78.38	62.00	60.78	65.73	64.70	32.31	34.50
	-	D_{le}	✓	✓	✓	✓	38.31	60.48	49.77	68.29	51.28	78.60	60.02	58.11	64.17	62.21	26.06	31.49
	IoU-Smooth L1 Loss	D_{oc}	✓	×	×	×	**44.32**	63.03	51.25	72.78	**56.21**	77.98	**63.22**	61.26	66.99	64.61	34.17	36.23
	Modulated Loss	D_{oc}	✓	×	×	×	42.92	67.92	52.91	72.67	53.64	**80.22**	58.21	61.21	66.05	63.50	33.32	34.61
	CSL	D_{le}	✓	×	×	✓	42.25	**68.28**	54.51	72.85	53.10	75.59	58.99	60.80	67.38	64.40	32.58	35.04
	DCL (BCL)	D_{le}	✓	×	×	×	41.40	65.82	**56.27**	**73.80**	54.30	79.02	60.25	**61.55**	**67.39**	**65.93**	**35.66**	**36.71**
	GWD	D_{oc}	×	×	×	×	**44.07**	**71.92**	**62.56**	**77.94**	**60.25**	**79.64**	**63.52**	**65.70**	**68.93**	**65.44**	**38.68**	**38.71**
R^{3}Det	-	D_{oc}	✓	✓	✓	×	44.15	**75.09**	72.88	**86.04**	56.49	82.53	61.01	68.31	70.66	67.18	**38.41**	**38.46**
	DCL (BCL)	D_{le}	✓	×	×	×	**46.84**	74.87	**74.96**	85.70	**57.72**	**84.06**	**63.77**	**69.70**	**71.21**	**67.45**	35.44	37.54
	GWD	D_{oc}	×	×	×	×	**46.73**	**75.84**	**78.00**	**86.71**	**62.69**	**83.09**	**61.12**	**70.60**	**71.56**	**69.28**	**43.35**	**41.56**

- AP on different objects and mAP on DOTA.

	Method	Backbone	MS	PL	BD	BR	GTF	SV	LV	SH	TC	BC	ST	SBF	RA	HA	SP	HC	mAP$_{50}$
Two-stage methods	ICN (Azimi et al., 2018)	R-101	✓	81.40	74.30	47.70	70.30	64.90	67.80	70.00	90.80	79.10	78.20	53.60	62.90	67.00	64.20	50.20	68.20
	RoI-Trans. (Ding et al., 2019)	R-101	✓	88.64	78.52	43.44	75.92	68.81	73.68	83.59	90.74	77.27	81.46	58.39	53.54	62.83	58.93	47.67	69.56
	CAD-Net (Zhang et al., 2019)	R-101		87.8	82.4	49.4	73.5	71.1	63.5	76.7	90.9	79.2	73.3	48.4	60.9	62.0	67.0	62.2	69.9
	SCRDet (Yang et al., 2019)	R-101	✓	89.98	80.65	52.09	68.36	68.36	60.32	72.41	90.85	87.94	86.86	65.02	66.68	66.25	68.24	65.21	72.61
	FADet (Li et al., 2019)	R-101	✓	90.21	79.58	45.49	76.41	73.18	68.27	79.56	90.83	83.40	84.68	53.40	65.42	74.17	69.69	64.86	73.28
	Gliding Vertex (Xu et al., 2020)	R-101		89.64	85.00	52.26	77.34	73.01	73.14	86.82	90.74	79.02	86.81	59.55	70.91	72.94	70.86	57.32	75.02
	Mask OBB (Wang et al., 2019)	RX-101	✓	89.56	**85.95**	54.21	72.90	76.52	74.16	85.63	89.85	83.81	86.48	54.89	69.64	73.94	69.06	63.32	75.33
	FFA (Fu et al., 2020)	R-101	✓	**90.1**	82.7	54.2	75.2	71.0	79.9	83.5	90.7	83.9	84.6	61.2	68.0	70.7	76.0	63.7	75.7
	APE (Zhu et al., 2020)	RX-101		89.96	83.62	53.42	76.03	74.01	77.16	79.45	90.83	87.15	84.51	67.72	60.33	74.61	71.84	65.55	75.75
	CenterMap (Wang et al., 2020a)	R-101	✓	89.83	84.41	54.60	70.25	77.66	78.32	87.19	90.66	84.89	85.27	56.46	69.23	74.13	71.56	66.06	76.03
	CSL (Yang & Yan, 2020)	R-152	✓	**90.25**	85.53	54.64	75.31	70.44	73.51	77.62	90.84	86.15	86.69	69.60	68.04	73.83	71.10	68.93	76.17
	RSDet-II (Qian et al., 2021)	R-152	✓	89.93	84.45	53.77	74.35	71.52	78.31	78.12	**91.14**	**87.35**	86.93	65.64	65.17	75.35	**79.74**	63.31	76.34
	SCRDet++ (Yang et al., 2020)	R-101	✓	90.05	84.39	55.44	73.99	77.54	71.11	86.05	90.67	**87.32**	87.08	69.62	68.90	73.74	71.29	65.08	76.81
Single-stage methods	PIoU (Chen et al., 2020)	DLA-34		80.9	69.7	24.1	60.2	38.3	64.4	64.8	**90.9**	77.2	70.4	46.5	37.1	57.1	61.9	64.0	60.5
	O^2-DNet (Wei et al., 2020)	H-104	✓	89.31	82.14	47.33	61.21	71.32	74.03	78.62	90.76	82.23	81.36	60.93	60.17	58.21	66.98	61.03	71.04
	P-RSDet (Zhou et al., 2020)	R-101	✓	88.58	77.83	50.44	69.29	71.10	75.79	78.66	90.88	80.10	81.71	57.92	63.03	66.30	69.77	63.13	72.30
	BBAVectors (Yi et al., 2020)	R-101	✓	88.35	79.96	50.69	62.18	78.43	78.98	87.94	90.85	83.58	84.35	54.13	60.24	65.22	64.28	55.70	72.32
	DRN (Pan et al., 2020)	H-104	✓	89.71	82.34	47.22	64.10	76.22	74.43	85.84	90.57	86.18	84.89	57.65	61.93	69.30	69.63	58.48	73.23
	R^{3}Det (Yang et al., 2021b)	R-152	✓	89.80	83.77	48.11	66.77	78.76	**83.27**	87.84	90.82	85.38	85.51	65.67	62.68	67.53	78.56	72.62	76.47
	PolarDet (Zhao et al., 2020)	R-101	✓	89.65	**87.07**	48.14	70.97	78.53	80.34	87.45	90.76	85.63	86.87	61.64	**70.32**	71.92	73.09	67.15	76.64
	S^{2}A-Net-DAL (Ming et al., 2020)	R-50	✓	89.69	83.11	55.03	71.00	78.30	81.90	**88.46**	90.89	84.97	**87.46**	64.41	65.65	76.86	72.09	64.35	76.95
	R^{3}Det-DCL (Yang et al., 2021a)	R-152	✓	89.26	83.60	53.54	72.76	**79.04**	82.56	87.31	90.67	86.59	86.98	67.49	66.88	73.29	70.56	69.99	77.37
	RDD (Zhong & Ao, 2020)	R-101	✓	89.15	83.92	52.51	73.06	77.81	79.00	87.08	90.62	86.72	87.15	63.96	**70.29**	**76.98**	75.79	**72.15**	77.75
	S^{2}A-Net (Han et al., 2021)	R-101	✓	89.28	84.11	**56.95**	**79.21**	**80.18**	82.93	**89.21**	90.86	84.66	**87.61**	**71.66**	68.23	**78.58**	78.20	65.55	**79.15**
	GWD (Ours)	R-152	✓	89.66	84.99	**59.26**	**82.19**	78.97	**84.83**	87.70	90.21	86.54	86.85	**73.47**	67.77	76.92	**79.22**	**74.92**	**80.23**